

## Review

## Electrochemical nitrogen reduction: an intriguing but challenging quest

Usman Bin Shahid,<sup>1,5</sup> Yifu Chen,<sup>2,5</sup> Shuang Gu,<sup>3,\*</sup> Whenzhen Li,<sup>2,\*</sup> and Minhua Shao<sup>1,4,\*</sup>

Ammonia plays an indispensable role in global agro-economics, chemical industries, energy carriers, and other diverse applications. To meet the demand for ammonia in these roles, the artificial synthesis of ammonia has traditionally relied on the well-established Haber–Bosch process that is commercially viable but energy intensive. Recently, the drive for sustainable alternatives has fueled interest in the development of electrochemical nitrogen reduction (eNRR) as a pathway for carbon-free ammonia synthesis. Nevertheless, research in the eNRR field remains elusive, partly because of the ominous presence of reactive nitrogen-containing species (Nr) and the lack of a thorough understanding of eNRR mechanistic. Herein, we provide an overview of efforts highlighting measures to avoid false positives and advancing mechanistic understanding of the eNRR process.

**Fixing nitrogen sustainably: the need for eNRR**

N<sub>2</sub> fixation to NH<sub>3</sub> is one of the most vital conversions critical to the propagation of life [1]. In the natural ecosystem, this fixation is facilitated by the enzyme ‘nitrogenase’, fixing roughly 40–100 million tons of N annually [2]. The advent of the ‘Haber–Bosch’ process revolutionized the chemical industry and fundamentally altered the balance of the global nitrogen cycle over the past century. With an annual NH<sub>3</sub> production of approximately 175 million tons [3], the Haber–Bosch process has dominated the industry despite its intense energy requirements (300–500 °C and 150–200 bar [4]) and its substantial release of greenhouse gases (1.44% of global CO<sub>2</sub> emissions) [5].

In this context, a sustainable alternative for NH<sub>3</sub> production has become a much sought-after research pursuit in the past decade [6]. A clean, energy abated, on-demand synthesis route for NH<sub>3</sub> can facilitate energy distribution and cut costs [6,7]. Among the several avenues explored, the most enticing has been the direct electrochemical reduction of N<sub>2</sub> to NH<sub>3</sub> (eNRR) under ambient conditions (Figure 1A) [8]. Although lithium-mediated (‘indirect eNRR’; Box 1) systems were reported decades earlier [9] for NH<sub>3</sub> synthesis with more consistent results, the strong reducing potentials, high energy consumption, and electrode/electrolyte instability limit their prospects as a scalable alternative [10].

Despite attracting immense research attention, recent eNRR research has raised more questions than it has answered [11–14]. The low NH<sub>3</sub> productivities (see Glossary) (Figure 1B), accompanied by the impact of numerous highly Nr, cast doubt on the reliability of some eNRR results [15–17]. Several existing reviews on eNRR [18,19] provide a comprehensive overview of published results; however, they rarely critically assess the mechanistic interpretations from advanced characterization methods and address the limitations of these techniques.

Herein, we aim to highlight the efforts in pursuit of direct eNRR over the recent years, addressing the challenges encountered in this tumultuous endeavor. In particular, we aim to highlight efforts

**Highlights**

The electrochemical nitrogen reduction (eNRR) offers a flexible and sustainable alternative to the well-established Haber–Bosch process to synthesize NH<sub>3</sub> in a distributed and on-demand manner.

Recent progress in the exploration of feasible eNRR systems has been impeded by inadequate understanding of eNRR mechanisms and plagued by interference from the unnoticed presence of reactive N-containing species.

As a crucial requirement for the design of control experiments in eNRR research, the quantitative <sup>15</sup>N<sub>2</sub> experiment provides the direct and most reliable evidence of the eNRR process.

Advanced *in situ* characterization techniques can deepen mechanistic understandings of the eNRR process, but attention should be devoted to the possible intervention of reactive nitrogen-containing species.

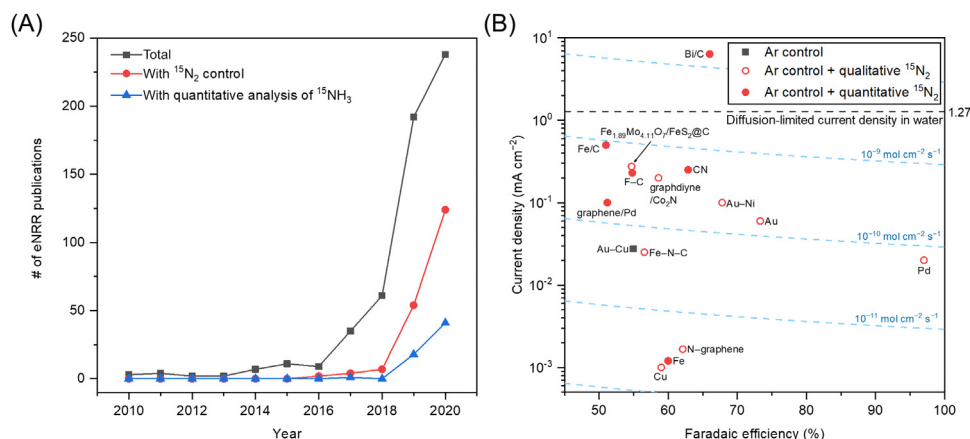
<sup>1</sup>Department of Chemical and Biological Engineering, The Hong Kong University of Science and Technology, Clear Water Bay, Kowloon, Hong Kong, China

<sup>2</sup>Department of Chemical and Biological Engineering, Iowa State University, Ames, IA, USA

<sup>3</sup>Department of Mechanical Engineering, Wichita State University, Wichita, KS, USA

<sup>4</sup>Energy Institute, Southern Marine Science and Engineering Guangdong Laboratory (Guangzhou), and Chinese National Engineering Research Center for Control and Treatment of Heavy Metal Pollution, The Hong Kong University of Science and Technology, Clear Water Bay, Kowloon, Hong Kong, China

<sup>5</sup>These authors contributed equally to this work.



\*Correspondence:  
 Shuang.Gu@wichita.edu (S. Gu),  
 wzli@iastate.edu (W. Li), and  
 kemshao@ust.hk (M. Shao).

### Trends in Chemistry

**Figure 1. Electrochemical nitrogen reduction (eNRR) research from 2010 to 2020.** (A) The number of eNRR publications by year. The data were obtained by searching for keywords in Web of Science (v.5.35) (and manual selection for careful inclusion). Publications focusing on theoretical work without experimental study are not counted here. The gray squares represent the total publications that performed eNRR measurements; the red circles represent the publications that used  $^{15}\text{N}_2$  for control experiments; the blue triangles represent the publications that conducted a quantitative analysis of produced  $^{15}\text{NH}_3$  from  $^{15}\text{N}_2$  experiments. (B) Steady-state current densities of the reported eNRR catalysts with >50% Faradaic efficiency (FE) towards  $\text{NH}_3$  [40,47,81,89–100]. The results from indirect eNRR (Li-mediated process) are not included. The gray squares represent the catalysts with Ar control experiments; the unfilled and filled circles represent the catalysts with qualitative and quantitative  $^{15}\text{NH}_3$  analysis from  $^{15}\text{N}_2$  experiments, respectively, besides Ar control experiments. The light-blue contour lines correspond to equal  $\text{NH}_3$  productivities ( $10^{-8}$ ,  $10^{-9}$ ,  $10^{-10}$ ,  $10^{-11}$ , and  $10^{-12}$  mol  $\text{cm}^{-2}$   $\text{s}^{-1}$ ). The black broken line represents the  $\text{N}_2$  diffusion-limited current density of eNRR in water ( $1.27$  mA  $\text{cm}^{-2}$ ), based on the estimation in [74]. Note: Strict caution is advised when considering  $\text{NH}_3$  yields reported in ' $\mu\text{g h}^{-1}$   $\text{mg}_{\text{cat}}^{-1}$ ' since this number can easily be inflated using a low  $\text{mg}_{\text{cat}}$  value and can sometimes be misleading.

#### Box 1. Indirect eNRR: a lithium-mediated approach

In parallel with the direct eNRR process, indirect eNRR, enabled by lithium mediation, can also convert  $\text{N}_2$  to  $\text{NH}_3$  under mild conditions. The lithium-mediated indirect eNRR process comprises the following key steps: electroreduction of  $\text{Li}^+$  [or the  $\text{Li}(\text{I})$  salt] to generate metallic Li; the spontaneous combination reaction between metallic Li and  $\text{N}_2$  to form  $\text{Li}_3\text{N}$ ; and the hydrolysis of  $\text{Li}_3\text{N}$  with a proton carrier (e.g., water) to form  $\text{NH}_3$  and  $\text{Li}^+$  or a  $\text{Li}(\text{I})$  salt, completing the catalytic cycle (Figure 1). The earliest reports on the strategy of indirect eNRR date back to 1930 by Fichter and colleagues [70], and it was then revived in the early 1990s by Tsuneto and colleagues [9,71]. More recently, interest in the indirect eNRR process was reignited by McEnaney and colleagues [72]. In the indirect eNRR process, the FE under ambient pressures can reach up to 19% at a current density of  $8$  mA  $\text{cm}^{-2}$  [73], while elevation of the  $\text{N}_2$  pressure can promote the FE to 29%, albeit at a lower current density ( $2$  mA  $\text{cm}^{-2}$ ) [74]. A more recent study by Suryanto and colleagues [34] reported an enhanced efficiency of 69% with an  $\text{NH}_3$  productivity of  $53$  nmol  $\text{s}^{-1}$   $\text{cm}^{-2}$  by replacing the traditional sacrificial proton source (i.e., ethanol) with a recyclable phosphonium salt.

Tetrahydrofuran (THF)-based solvent was initially used as the electrolyte to conduct the indirect eNRR by Tsuneto and colleagues [9]. Shortly afterwards, Ito and Goto [75] demonstrated the feasibility of using molten salts as the electrolyte, leading to one of the highest reported  $\text{NH}_3$  productivities. Later, McPherson and colleagues [76] introduced lithium hydride as a catalytic mediator to enhance the performance of molten chloride systems, validating their results through quantitative  $^{15}\text{N}_2$  experiments.

Although the lithium-mediated indirect eNRR successfully overcomes the challenges encountered in the direct eNRR, it creates new problems. For instance, the working electrode used in the indirect eNRR often suffers instability issues, as the potential at the working electrode can deteriorate over time (i.e., negatively drifting resulting in increased energy consumption). The deterioration of the working electrode was attributed to the gradual accumulation of a Li-containing passivation layer, hypothesized to be a consequence of the undesired reduction of some species within the electrolyte. Another issue lies in the high energy consumption of the indirect eNRR process, due largely to the extreme working potential required to reduce  $\text{Li}^+$ . So far, the state-of-the-art energy efficiency of the indirect eNRR process is less than 7% [10].

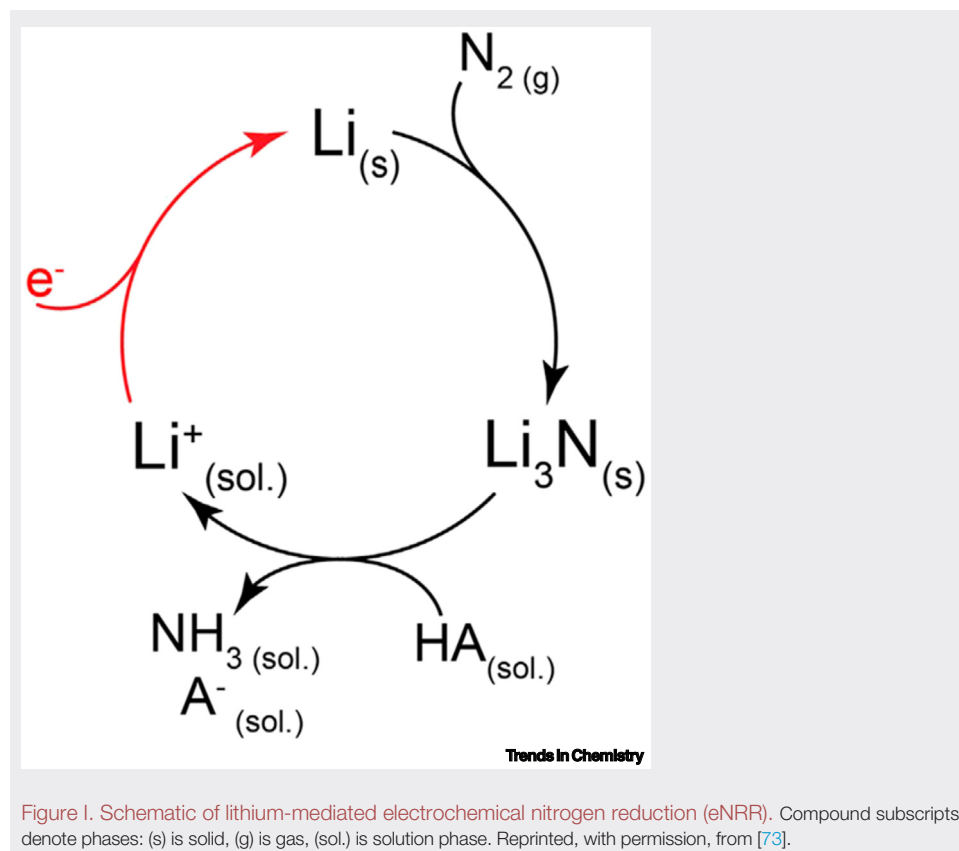


Figure 1. Schematic of lithium-mediated electrochemical nitrogen reduction (eNRR). Compound subscripts denote phases: (s) is solid, (g) is gas, (sol.) is solution phase. Reprinted, with permission, from [73].

that have played a critical role in helping researchers avoid false positives and pitfalls by identifying and eliminating Nr in the eNRR experimental protocol. Moreover, we extend the past developments in the design of **control experiments**, improving the  $^{15}\text{N}_2$  circulation system so that the quantitative assessment of  $\text{NH}_3$  origins can be significantly economized and facilitated. Furthermore, we also endeavor to present a critical assessment of mechanistic studies probing eNRR and discuss the limitations of the tools used for the purpose.

### Potential impact of Nr in eNRR research

Careful implementation of control experiments is an essential requirement of eNRR research [20]. An exhaustive review of recent eNRR research has shown that tracing the origin of the  $\text{NH}_3$  produced takes considerably more effort than observing the  $\text{NH}_3$  formation itself [5,14]. In essence, this unique challenge is due to the widespread presence of Nr (Figure 2A), whose electroreduction exclusively favors  $\text{NH}_3$  production in many cases [21–23]. Among all reported eNRR systems, the proportion of converted  $\text{N}_2$  is indiscernibly small, making the verification of ‘successful  $\text{N}_2$  fixation’ solely dependent on meticulous quantification of the  $\text{NH}_3$  produced at a subtle level, which is the sum of the contributions from all possible sources.

The existence of Nr was often overlooked in the earlier stage of eNRR research but has drawn appreciable attention recently [13,16]. Depending on its occurrence, Nr can originate from two sources: (i) the external and adventitious sources that may intrude into eNRR systems, such as human breath [17], ambient air [17], chemical containers [24], and nitrile gloves [16]; and (ii) internal and indigenous sources that could be heavily involved in eNRR systems, such as the feeding

### Glossary

#### Associative and dissociative mechanisms:

two mechanisms of  $\text{NH}_3$  synthesis. In the associative mechanism, the first activation step involves the hydrogenation of  $\text{N}_2$  molecules (e.g., in enzymatic processes). In the dissociative mechanism, the breaking of the  $\text{N}=\text{N}$  triple bond occurs first (e.g., in the Haber–Bosch process).

#### Attenuated total reflection–Fourier transform IR (ATR–FTIR) spectroscopy:

a sampling technique that can *in situ* probe the layers of adsorbed species at a solid–liquid interface and provides the information of IR adsorption related to specific functional groups and chemical structure.

#### Control experiments:

in the eNRR research, the crucial experiments are carried out with the controlled feeding gas (both argon and  $^{15}\text{N}_2$ ), while keeping all other conditions identical to the electrolysis with  $^{14}\text{N}_2$  as feeding gas.

#### Differential electrochemical mass spectrometry (DEMS):

an analytical technique, combining electrochemical experimentation with mass spectrometry, allowing for *in situ*, mass-resolved observation of gaseous or volatile species in electrochemical reactions.

**Faradaic efficiency (FE):** the efficiency with which electrical charge is transferred towards a given electrochemical reaction leading to target products.

#### Mars–van Krevelen (MvK) mechanism:

a characteristic mechanism with which some products carry one or more constituents of the catalysts’ lattice, when leaving the surface of the catalyst. For the eNRR process on transition metal nitrides, a proposed MvK mechanism involves the removal (reduction) of a surface nitride N atom to  $\text{NH}_3$ , and then, the created N vacancy is replenished by  $\text{N}_2$  molecule to complete the catalytic cycle.

**$\text{NH}_3$  productivity:** the rate of  $\text{NH}_3$  production normalized by the geometric area of electrode (unit:  $\text{mol NH}_3 \text{ cm}^{-2} \text{ s}^{-1}$ ).

**NMR spectroscopy:** a spectroscopic technique critically used in the eNRR research, in which the characteristic triplet and doublet peaks for  $^{14}\text{NH}_4^+$  and  $^{15}\text{NH}_4^+$  are well identifiable with  $\mu\text{M}$ -level detection limit.

#### Primary bond-dissociation energy:

a measure of the strength for a chemical bond R–X, defined as the standard

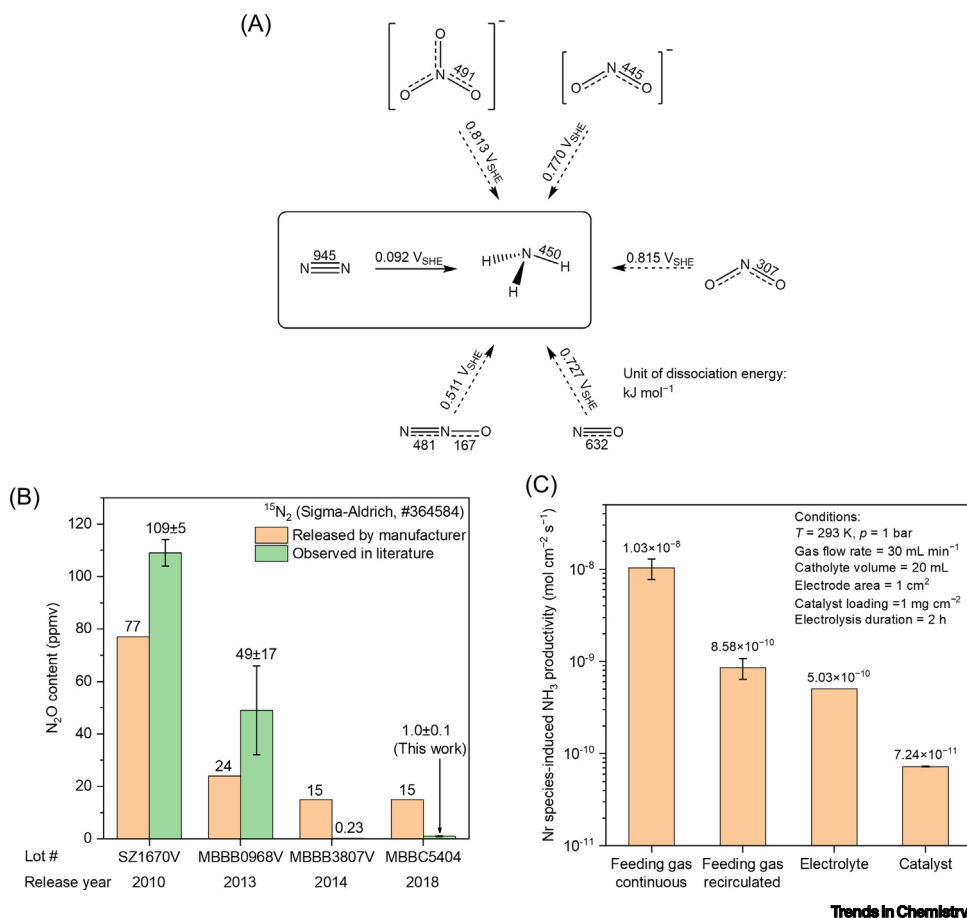


**Figure 2.** Potential impact of reactive nitrogen-containing species (Nr) in electrochemical nitrogen reduction (eNRR) measurement. (A) **Primary bond-dissociation energies** (enthalpies;  $\text{kJ mol}^{-1}$ ) and standard reduction potentials ( $V_{\text{SHE}}$ ) of some common N-containing species, including  $\text{NO}_3^-$  (aqueous),  $\text{NO}_2^-$  (aqueous),  $\text{NO}_2$  (gas),  $\text{NO}$  (gas), and  $\text{N}_2\text{O}$  (gas). Data obtained from [101]. (B)  $\text{N}_2\text{O}$  content in different batches of  $^{15}\text{N}_2$  (Sigma-Aldrich, product #364584) on the official certificate of analysis (COA) and observed experimentally [14,25].  $\text{N}_2\text{O}$  (lot #MBBC5404) was determined by gas chromatography [102]. (C) Calculated  $\text{NH}_3$  productivity from non- $\text{N}_2$  sources, including Nr in the feeding gas, electrolyte, and catalyst, based on the highest reported Nr content in the literature:  $496 \pm 127$  ppmv Nr (as  $\text{NO}_x$ ,  $\text{NH}_3$ , and  $\text{N}_2\text{O}$ ) in a commercial  $^{15}\text{N}_2$  gas [25],  $0.181$  mM Nr (as  $\text{NO}_3^-$  and  $\text{NO}_2^-$ ) in a  $0.5$  M  $\text{Li}_2\text{SO}_4$  solution [26], and  $7297 \pm 99$  ppm Nr (as nitrides) in an Fe catalyst [13]. Other assumed conditions for the calculation are specified in the figure except for the case of ‘feeding gas recirculated’, in which a total gas volume of  $300$  ml was assumed. Abbreviation: SHE, standard hydrogen electrode.

gases [25], supporting electrolytes [26], catalysts [13], and membranes [27]. The impact of Nr from external/adventitious sources is generally difficult to quantify and is likely to be minor compared with the latter since it can be significantly alleviated by following the step-by-step experimental procedures as suggested in [14,28].

The most common forms of internal/indigenous Nr have been identified as nitrate ( $\text{NO}_3^-$ ), nitrite ( $\text{NO}_2^-$ ), and ammonium ( $\text{NH}_4^+$ ), which have been detected in solution balanced or bubbled with  $^{15}\text{N}_2$  gas [16,25], lithium salts [26], metal oxides [13], and metallic iron catalysts [13] from various mainstream chemical suppliers. A less-noticed gaseous impurity is  $\text{N}_2\text{O}$ , which was confirmed as an obstinate contaminant in the  $^{15}\text{N}_2$  gas produced by Sigma-Aldrich at varying

enthalpy change of the fission:  $\text{R-X} \rightarrow \text{R} + \text{X}$ . Here, ‘primary’ is referred to as the first dissociated chemical bond in species that contain multiple identical bonds.

**Surface-enhanced IR absorption spectroscopy (SEIRAS):** a surface-sensitive technique that exploits the electromagnetic properties of nanostructured metal films to enhance the vibrational bands of a molecular adlayer.

**X-ray absorption spectroscopy (XAS):** a measurement technique for determining the geometric and electronic structures in a sample by its X-ray absorption characteristics, usually performed at synchrotron radiation facilities.

levels, from  $109 \pm 5$  ppmv in a batch produced in 2010 [25] to  $1.0 \pm 0.1$  ppmv in a batch produced in 2018 (Figure 2B).

Based on the highest content of Nr reported in the literature [13,25,26], we calculated the maximum  $\text{NH}_3$  productivities stemming from these Nr in different sources (Figure 2C), with key assumptions based on the typical conditions for eNRR measurement (detailed in the figure legend). The calculation results are the upper limits, but they can be informative in alerting the reader to the severity of the potential impact, as the values exceed many reported eNRR productivities (Figure 1B). In agreement with the recent analysis by Choi and colleagues [14], a recirculated gas with a fixed volume (detailed in the next section) can reduce the impact of Nr from 10.3 to  $0.9 \text{ nmol cm}^{-2} \text{ s}^{-1}$  on the  $\text{NH}_3$  productivity compared with a continuous flow of feeding gas.

### Suggested practices for eNRR research

#### Eliminating Nr from the eNRR system

The preceding discussion highlights the necessity of efficient cleansing procedures to limit the impact of Nr in eNRR systems. For this purpose, a cold trap containing freshly reduced Cu-based  $\text{deNO}_x$  catalyst [16] or a scrubbing solution containing alkaline  $\text{KMnO}_4$  [14] before the eNRR reactor can be used for gas cleansing. For simplicity and versatility, we recommend a two-stage gas scrubbing installation that comprises an alkaline  $\text{KMnO}_4$  solution and a dilute acid solution via porous spargers to remove any NO,  $\text{NO}_2$ , or  $\text{NH}_3$  [29] (Figure 3A). Our measurements with colorimetric tubes show that more than 99% of NO and  $\text{NO}_2$  can be removed when 100 ppmv NO or  $\text{NO}_2$  standard gas was fed through the installation.

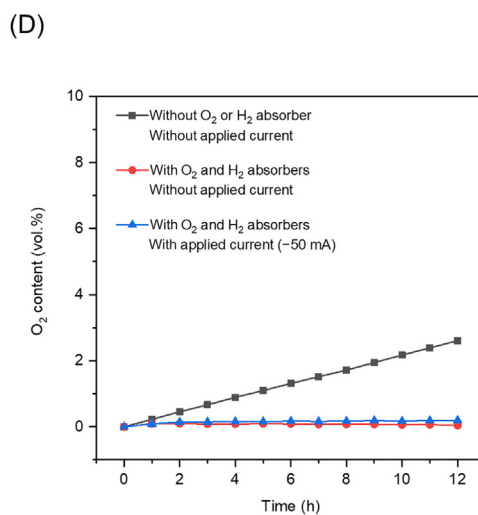
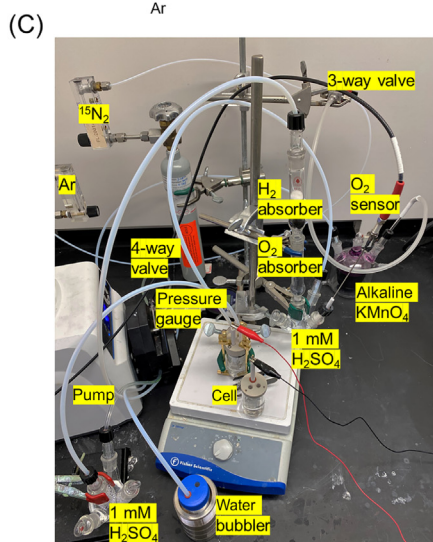
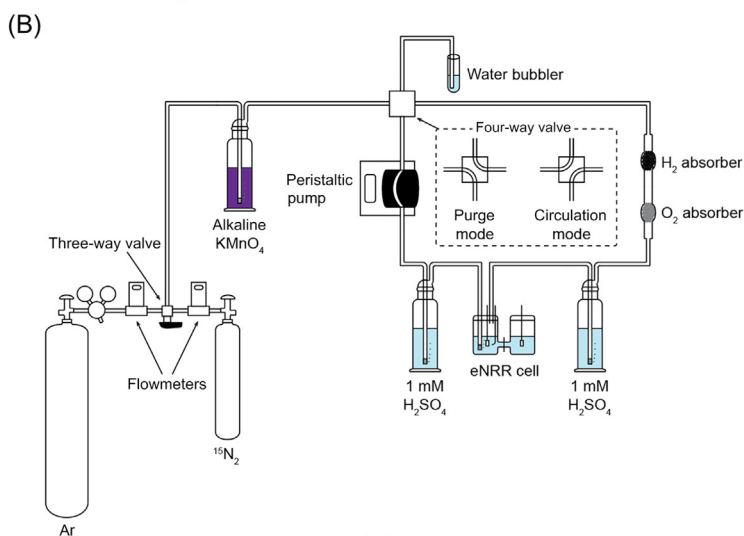
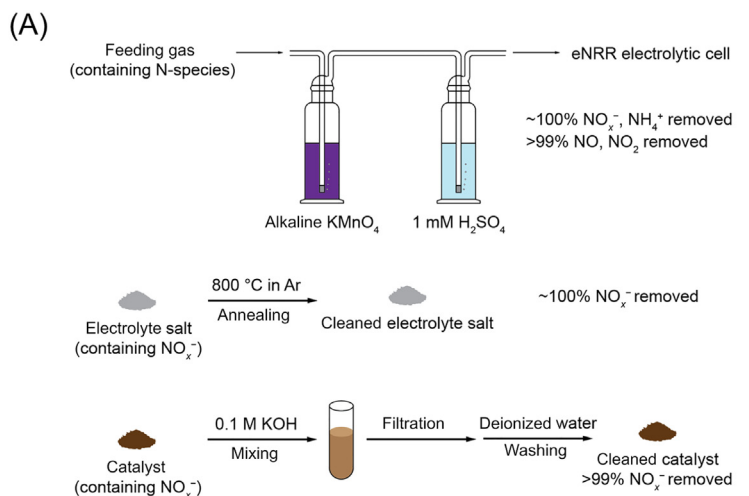
Nevertheless, we note that neither the  $\text{KMnO}_4$  scrubbing solution nor the  $\text{deNO}_x$  catalyst can remove  $\text{N}_2\text{O}$  efficiently, as evidenced by our gas chromatography test results and the results in [30,31]. To the best of our knowledge, no convenient method is currently available in laboratories for the rapid and efficient elimination of  $\text{N}_2\text{O}$  [31]. Hence, we reiterate that special attention should be given to the content of  $\text{N}_2\text{O}$  impurity in the gases used for eNRR, especially for  $^{15}\text{N}_2$ , which have had a high  $\text{N}_2\text{O}$  content in earlier batches.

For Nr from non-gas sources, a control experiment with Ar should be a good indicator of the baseline contamination level. Methods based on HPLC [32] or UV-visible (UV-Vis) spectroscopy [33] are available for the quantification of  $\text{NO}_3^-$  and  $\text{NO}_2^-$ . Once identified, these soluble anions can be effectively removed by heat treatment [26] or alkaline washing [13].

We again stress that, despite proper cleansing procedures in place, it is still necessary to examine the remaining Nr (if any) to confirm the efficacy of Nr removal. In this regard, Suryanto and colleagues provided an exemplary practice in their recent work on Li-mediated  $\text{N}_2$  fixation [34], including a set of rigorous and quantitative measurements with different gases (Ar,  $^{14}\text{N}_2$ ,  $^{15}\text{N}_2$ ), screening and assessing Nr in the electrolyte and gases under different testing conditions.

#### Presenting an effective and affordable gas circulation system for eNRR

$^{15}\text{N}_2$ -based **NMR spectroscopy** can probe the origin of N sources for  $\text{N}_2$  fixation directly. The significance of obtaining such direct evidence for  $\text{N}_2$  fixation was underestimated in the earlier research stage (as shown in Figure 1A) due to the high cost of  $^{15}\text{N}_2$ , which also prompted many researchers to use a low-volume injection of  $^{15}\text{N}_2$  in an Ar-presaturated environment for eNRR. However, the injected  $^{15}\text{N}_2$  gas does not attain instant equilibrium with the surrounding solution [35], which may affect the measured eNRR performance; concentration of  $^{15}\text{NH}_4^+$  is often required as an additional step to obtain a detectable signal. By cycling a fixed volume of gas in a closed loop, the costly  $^{15}\text{N}_2$  can be more effectively utilized, allowing a more accurate



Trends in Chemistry

(See figure legend at the bottom of the next page.)

evaluation of  $^{15}\text{NH}_3$  productivities while suppressing the impact of Nr. A flowing  $^{15}\text{N}_2$  gas is also required to rigorously examine the eNRR performance in novel flow electrolyzers with gas diffusion electrodes (GDEs) [36].

While such a gas circulation system has been adopted in a few publications [13,16,31,37], it remains uncommon in the eNRR field. By taking advantage of prior systems, here we propose an effective and affordable gas circulation system for eNRR research, as illustrated in Figure 3B and its legend. A peristaltic pump is used for contact-free control of the gas flow to avoid the introduction of Nr from the pump. PTFE tubing should be used to build the circulation loop to minimize the leakage of circulated gas and ambient air [38]. A commercial  $\text{O}_2$  absorber and a laboratory-made  $\text{H}_2$  absorber are incorporated into the circulation system to alleviate  $\text{O}_2$  accumulation (via ambient air permeation) and  $\text{H}_2$  accumulation (via the electrochemical side-reaction), respectively.

The operational stability of the gas circulation system was examined with an  $\text{O}_2$  sensor and a pressure gauge (Figure 3C). In a 12-h operation without an  $\text{O}_2$  or  $\text{H}_2$  absorber, we observed that the  $^{14}\text{N}_2$  content in the loop increased over time (from 0 at the start to 3.6 vol% at the end of the 12-h operation), possibly due to the permeation of ambient air into the loop (Figure 3D and legend). Therefore, in the actual  $^{15}\text{N}_2$  experiment, one should expect a small signal of  $^{14}\text{NH}_4^+$  in the NMR spectrum originating from this permeated  $^{14}\text{N}$  in addition to the inherent  $^{14}\text{N}$  present in the commercial  $^{15}\text{N}_2$  gas (~2 atom%) and other Nr. Overall, the  $\text{O}_2$  level increased steadily but remained low in such a period of operation. By contrast, with both  $\text{O}_2$  and  $\text{H}_2$  absorbers installed in the loop, no considerable increase in  $\text{O}_2$  content (<0.2 vol%) or pressure (<0.02 bar) was detected during the same operation time (12 h), even when a substantial amount of  $\text{H}_2$  is generated by electrolysis at -50 mA. These results confirm the efficacy of both absorbers in alleviating  $\text{O}_2$  and  $\text{H}_2$  accumulation in the gas circulation system, which is expected to operate stably for much longer durations sufficient for eNRR research needs.

The versatile  $^{15}\text{N}_2$  gas circulation system can also be equipped with different electrolytic cells (including H-type cells, flow cells, and undivided cells) while allowing convenient regulation of the gas flow rate by modulating the pump motor speed. Furthermore, it can also be modified for mechanistic studies by isotope-sensitive characterization techniques, such as **surface-enhanced IR absorption spectroscopy (SEIRAS)**, **differential electrochemical mass spectrometry (DEMS)**, and isotopic scrambling, to elucidate valuable mechanistic insights.

## Progress in mechanistic understanding of eNRR

### eNRR mechanistic studies and gauging criteria

The plausibility of the eNRR remains manifest in the natural  $\text{N}_2$  fixation by ‘nitrogenase’ under ambient conditions. However, the complex nature of the nitrogen-reduction process necessitates a thorough mechanistic understanding to enable an efficient artificial process under similar mild

**Figure 3. Suggested practices in conducting electrochemical nitrogen reduction (eNRR) research.** (A) Suggested procedures for cleansing the feeding gas, electrolyte salt, and catalyst, based on [13,26,29]. The content of both NO and  $\text{NO}_2$  in standard gases (100 ppmv in  $\text{N}_2$ , fed at  $30 \text{ ml min}^{-1}$ ) was below the 1-ppmv detection limit of the colorimetric tube (Kitagawa America) after two-stage scrubbing. (B) Schematic illustration of the gas circulation system, in which a three-way valve controls the feeding gas and a four-way valve controls the operating mode. An alkaline  $\text{KMnO}_4$  solution removes any  $\text{NO}_x$  impurity in the gas supply. The circulation loop contains a peristaltic pump, an acid scrubber before the cell, the eNRR cell, a  $\text{NH}_3$  collector (acidic), an  $\text{O}_2$  absorber (ShieldPro), and a  $\text{H}_2$  absorber (10%  $\text{Ag/MnO}_2$  [103]). The loop is connected by PTFE tubing except for the pump segment where soft tubing (Tygon® Chemical) is used. Detailed operation procedures of the gas circulation system are described in [16]. (C) Photograph of the gas circulation system, with an  $\text{O}_2$  sensor probe (NeoFox) and a pressure gauge (0–30 psi) to monitor the operational stability. (D)  $\text{O}_2$  content under different conditions during 12 h of  $^{15}\text{N}_2$  circulation. Without the absorbers,  $\text{O}_2$  content increased at a rate of  $0.22 \text{ vol}\% \text{ h}^{-1}$  due to the slow permeation of ambient air at the soft tubing. The estimated rate of ambient  $^{14}\text{N}_2$  entering the system is  $0.32 \text{ vol}\% \text{ h}^{-1}$ , based on the relative permeabilities of  $\text{N}_2$  and  $\text{O}_2$  [104].



conditions. In recent years, several exciting approaches have emerged, focusing on elucidating the eNRR mechanism. These approaches include *in situ* spectroscopic studies, such as IR spectroscopy [e.g., SEIRAS, **attenuated total reflection–Fourier transform IR (ATR-FTIR)** spectroscopy], DEMS, **X-ray absorption spectroscopy (XAS)**, and **Raman spectroscopy** (Figure 4D–F), alongside theoretical modeling approaches based on density functional theory (DFT). The ultimate objective is to identify reaction intermediates involved in the transformation of  $N_2$  to  $NH_3$  to help elucidate the reaction mechanism as either ‘**associative**’ or ‘**dissociative**’ (Figure 4B). The mechanistic knowledge of reaction steps can aid the design of active catalysts that favor the formation of such intermediates and allow rapid and selective conversion of  $N_2$  to  $NH_3$ . Moreover, it could also serve as *prima facie* evidence of direct  $N_2$  fixation over the catalyst.

However, as discussed earlier, the ominous presence of Nr prompts inquiry about whether the observed  $NH_3$  is a product of eNRR or the more facile reduction of Nr [e.g., electrochemical reduction of  $NO_3^-$  (eNO<sub>3</sub>RR)]. Therefore, we first set out to identify studies that fulfill the requirements for a ‘genuine’ eNRR mechanistic study. For this, we subjected an exhaustive list of relevant studies (Table S1 in the supplemental information online) that used either *in situ* or *ex situ* characterization techniques to validate any mechanism to the following criteria (including those adopted by Choi and colleagues [14]).

- (i) Are there any controls to limit the Nr present in the experimental protocols?
- (ii) Has the efficiency of these purification measures, as outlined in [14], been evaluated?
- (iii) Have the characteristic signals for Nr been adequately screened in exclusive control experiments?
- (iv) Is the focus on the direct identification of  $N_2H_y$  intermediates or reliant on indirect evidence to substantiate the findings?
- (v) Are the experiments using  $^{15}N_2$  reliable and sufficient to confirm the key results?

In summary, of the 37 studies that qualified as ‘mechanistic’ studies, only five [31,39–42] demonstrated proper controls to limit these Nr adequately [i.e., satisfying both criterion (i) and criterion (ii)] and one partially satisfied both requirements. However, none of these studies reported screening of the characteristic signals of the most probable Nr. Although most of these studies corroborate their results with  $^{15}N_2$  tests, *in situ* characterizations were never repeated with  $^{15}N_2$ .

### *In situ* IR spectroscopy

Among the several *in situ* characterization tools mentioned earlier, *in situ* IR spectroscopy has been the most popular tool for investigating eNRR intermediates. The seminal work by Yao and colleagues [43] was the earliest endeavor using SEIRAS to study the eNRR reaction mechanism on an Au thin film and set a precedent for subsequent studies. In the past, the same technique was used to identify intermediates and their characteristic bands for either  $NO_x$  reduction or  $NH_3$  oxidation over various catalysts [9], which proved helpful in identifying eNRR intermediates. In their investigation, under electrode potentials more negative than  $-0.10 V_{RHE}$  ( $V_{RHE}$ : V vs. RHE, hereinafter), distinct peaks in the range  $1100$ – $1500\text{ cm}^{-1}$  were observed on the Au surface. Of particular interest were the peaks at  $1450$ ,  $1298$ , and  $1109\text{ cm}^{-1}$ , as these allude to the presence of ‘H–N–H bending’, ‘ $-NH_2$  wagging’, and ‘N–N stretching’, respectively, related to  $N_2H_y$  moieties (Figure 4B).

In a subsequent study, the presence of adsorbed  $N_2H_y$  species was again confirmed under increasingly negative electrode potentials in acidic media during eNRR on Ru [44] and Rh [45].

that XAS probes, and (iii) three different XAS detection modes – transmission mode, fluorescence mode, and electron yield mode. (F) Schematic diagram of modern *in situ* (i) electrochemical Raman spectroscopy (EC-RS) and (ii) surface-enhanced RS (SERS) setups. (iii) *In situ* RS for probing of the solvent, intermediate, and catalyst state. Reprinted, with permission, from [52,105–108]. Abbreviations: CE, counter electrode; RE, reference electrode; WE, working electrode.

Rh was further studied using SEIRAS for eNO<sub>3</sub>RR, in which Yao and colleagues [45] observed that both follow the same mechanistic pathway with an N<sub>2</sub>H<sub>y</sub> intermediate. SEIRAS coupled with DEMS confirmed the presence of an 'N=N' moiety, and the pulse signal of diazene (N<sub>2</sub>H<sub>2</sub>) served as compelling evidence for the involvement of N<sub>2</sub>H<sub>2</sub> in the reduction pathways of both eNO<sub>3</sub>RR and eNRR. Other studies (Table S1 in the supplemental information online) that use IR spectroscopy have primarily relied on the presence of the same bands identified by Yao and colleagues [43–45] to justify the possible associative mechanism for eNRR on their catalyst. However, the absence of measures to limit the impact of Nr remains a paramount concern in these studies, leaving the eNRR mystery unresolved.

Nevertheless, a few more recent studies have demonstrated appropriate controls and their corresponding efficiencies, thus limiting the impact of Nr in their eNRR tests. Notably, Liu [39,42,46] and Wang [31,40,47], with colleagues' work on enhancing nitrogen availability to the catalyst's surface while suppressing the hydrogen evolution reaction (HER) via the salting-out effect, are a paradigm of efforts in a proper direction. Wang and colleagues [31] observed two peaks at 1298 and 1109 cm<sup>-1</sup> attributed to '-NH<sub>2</sub> wagging' and 'N-N stretching' similar to past studies, although in a different electrolyte containing 10 M LiCl. The results demonstrated suppression of HER at high LiCl concentrations, consequently paving the way for eNRR by making N<sub>2</sub> available at the electrode surface.

Similarly, recent work by Wang and colleagues [48] investigated the role of fluorine vacancies as promoters for eNRR by tuning the charge distribution at the catalytic site. The fluorine vacancy is of particular interest, as it deviates from the traditionally explored oxygen vacancies and yet exhibits a moderate **Faradaic efficiency (FE)** (36%) and NH<sub>3</sub> productivity (0.13 nmol cm<sup>-2</sup> s<sup>-1</sup>) [48], with controls in place to remove Nr. However, their *in situ* study examined the available proton supply rather than identifying the typical N<sub>2</sub>H<sub>y</sub> intermediates in eNRR. Notwithstanding the progressive efforts, the ammonia yield rates have remained low.

#### *In situ* XAS exploring Mars–van Krevelen mechanism

This technique focuses on detecting structural changes at the catalyst surface rather than directly probing reaction intermediates, making it an indirect method for studying eNRR mechanisms; however, it is ideal for studying mechanisms involving structure-altering intermediates. A **Mars–van Krevelen (MvK) mechanism**, besides the conventional associative and dissociative mechanisms, has also been suggested for eNRR on transition-metal (TM) nitride (TMN) surfaces. It essentially involves reducing N atoms at the TMN surface to NH<sub>3</sub>, leaving behind an N vacancy subsequently replenished by an adsorbed N<sub>2</sub> molecule, thus sustaining the catalytic cycle (Figure 4C) [49]. Abghoui and colleagues [50,51] contend that the exothermic adsorption of N<sub>2</sub> on an N vacancy in contrast to the endothermic adsorption on pure TMs and clean TMNs makes the MvK mechanism highly favorable. Thus motivated, Yang [52] and Nash [53], with colleagues, used *in situ* XAS to investigate vanadium nitride (VN) and chromium nitride (CrN), which had been suggested previously [54,55] as promising candidates for eNRR. Their results suggested VN<sub>0.7</sub>O<sub>0.45</sub> and Cr<sub>2</sub>N, rather than pristine VN and CrN, to be the most active phases for eNRR via the MvK mechanism. In a follow-up study, Yang and colleagues [56] conducted an intriguing <sup>14</sup>N/<sup>15</sup>N exchange experiment to further validate the MvK mechanism. They hypothesized that the surface nitrogen atoms of a catalyst, once consumed during eNRR (i.e., MvK-based displacement), should, in principle, have traces of <sup>15</sup>N on the surface when a <sup>15</sup>N<sub>2</sub> feed is used. Reusing the same catalyst for eNRR but with <sup>14</sup>N<sub>2</sub> feed should release this surface <sup>15</sup>N. As a result, <sup>15</sup>NH<sub>4</sub><sup>+</sup> product can be realized when the second round of MvK displacement occurs under a <sup>14</sup>N<sub>2</sub> feed. The MvK mechanism was thus justified based on their results, albeit with a minimal number of active sites. However, the lack of rigorous protocols and questionable

### Box 2. Concurrent controversies over eNRR systems

Adventitious Nr have raised reasonable skepticism in reported eNRR systems, as those impurities may have led to many false positives. The discovery of the unexpected  $\text{NO}_x$  species from commercial  $\text{Fe}_2\text{O}_3$  catalysts [13] has resulted in the retraction of an article from *Science* [77]. Such a retraction is highly commendable as it demonstrates the integrity much needed in scientific research to make meaningful progress. At the same time, many others have maintained their ground despite contradictory correspondences [78] and articles [79,80].

The most controversial case is perhaps that of Bi. Although its intrinsic disfavor for HER makes it an appealing candidate for eNRR, the research community has yet to reach a consensus over its true catalytic activity. Hao and colleagues [81] reported nanostructured Bi as a promising candidate, with one of the highest  $\text{NH}_3$  productivities ( $14.4 \text{ nmol cm}^{-2} \text{ s}^{-1}$ ) in the field. However, a subsequent correspondence by Choi and colleagues [78] questioned Bi's functionalities as no measurable eNRR activity was observed in their study, contrary to Hao's findings. Nevertheless, Yao and colleagues [82] used *in situ* Raman spectroscopy to study the structural transformation of the Bi-based eNRR catalyst. They attributed the  $\text{NH}_3$  production to structural changes in the Bi-based metal-organic framework (Bi-MOF) nanorods when subjected to reducing potentials, indicating that the Bi-MOF nanorods were reduced to metallic Bi nanoparticles that dominated the electrode surface. Several other studies [83–85] have reported the propensity of Bi for eNRR; however, the absence of control over Nr, in addition to the disparity in performance results between these studies, raises serious concerns.

Akin to Bi, TMNs have also attracted support and criticism alike for their prospects as eNRR catalysts. The electrochemically induced MvK mechanism has often been used to justify the observed activity, as discussed earlier. However, the reader should be aware that two separate studies challenged the functionalities of VN catalysts [79,80]. After a series of experiments with robust testing protocols to limit adventitious Nr, Du and colleagues [80] found that VN was not electrocatalytically active for eNRR. They suggested that the detected  $\text{NH}_3$  product may instead have originated from an irreversible release of lattice nitrogen. Manjunatha and colleagues [79] also observed that significant amounts of vanadium and nitrogen had leached into electrolytes when the VN was subjected to a 12-h exposure without electrochemical treatment.

Likewise, catalysts derived from nitrogen-containing precursors [86] have also emerged as controversial materials for eNRR, because of the possibility of lattice nitrogen being released as  $\text{NH}_3$  [87].

It is still early to call the debate settled; however, as delineated in recently published protocols [16,88], prudent research practices can surely help the research community reach a consensus.

stability of TMNs under the experimental conditions have stirred debate on the propensity of these TMNs for eNRR (Box 2).

### Capabilities and limitations of eNRR mechanistic characterization

As is the case for all instruments, notwithstanding their capabilities, they still have limitations beyond which their application is futile. The mechanistic studies discussed thus far have focused on techniques that can detect any 'N-H' or related intermediates. However, given the limiting performance of eNRR on a multitude of catalysts and the extremely low productivities [57], the signal for any intermediate of interest is extremely weak in principle. With this lingering uncertainty, it is of paramount importance that the capabilities of these instruments in reliably detecting these intermediates at extremely low concentrations be first ascertained. This critical aspect has remained vastly ignored thus far.

In some studies, *in situ* surface characterization of catalysts is used to correlate eNRR activity indirectly, while few endeavors probe  $\text{N}_2\text{H}_y$  intermediates as direct evidence for the eNRR process. For the indirect approach using *in situ* characterization tools (like *in situ* XAS or XRD), there remains plenty of room for speculation and assumption when interpreting characterization results (especially when lacking proper controls for Nr). At the same time, the direct approach based on  $\text{N}_2\text{H}_y$  intermediates also demands extreme caution, as the same  $\text{N}_2\text{H}_y$  moieties could be intermediates of two entirely different reactions: eNO<sub>3</sub>RR or possibly the eNRR (Figure 4A–C) [45]. Notwithstanding the capabilities of these *in situ* characterization tools, the results of these studies should be interpreted with great prudence, subject to thorough validation of the link between these intermediates (and surface changes) with either eNRR or eNO<sub>3</sub>RR.

Another aspect of instrument limitation that requires due consideration is the influence of external factors on the measured values. Taking FTIR as an example, there are known limitations. First, monoatomic gases (e.g., Ar), homonuclear diatomic molecules (e.g., O<sub>2</sub>, N<sub>2</sub>), and monoatomic ions (e.g., Na<sup>+</sup>, Cl<sup>-</sup>) are oblivious to IR exposure and generally undetectable in FTIR scans. Nevertheless, monoatomic ions (or strongly adsorbed diatomic molecules [58] with altered molecular symmetry) can sometimes strongly influence the spectra of surrounding solvent molecules, making it difficult to ascertain their identity [59]. Second, for a complex mixture, there remains a strong possibility that the signal of another dominant species may camouflage an undesired species. For example, the menacing presence of NO<sub>x</sub> ('NO': 1730 and 1603 cm<sup>-1</sup>; 'ads-NO<sub>3</sub><sup>-</sup>': 1547–1568 cm<sup>-1</sup>) [60] can be easily masked by the broad and intense peaks of H<sub>2</sub>O (3300 and 1633 cm<sup>-1</sup>) [43]. Therefore, a thorough investigation of possible contaminants and their characteristic signals must be conducted. Most importantly, the sensitivity of the characterization tool for the intended purpose must also be thoroughly investigated. FTIR, for example, can only detect NH<sub>3(aq)</sub> concentrations beyond 10 400 ppm [61] in the bulk liquid phase, while species adsorbed on the catalyst can reliably detect at much smaller concentrations facilitated by the applied overpotential.

*In situ* surface characterization techniques can also help to reveal structural changes, especially for a displacement-based mechanism like MvK. However, researchers have mostly resorted to 'deductive reasoning' to justify the existence of MvK-based eNRR instead of pursuing direct evidence of atomic displacement on the surface. The isotopic exchange reactions on the catalyst surface following an MvK mechanism should, in principle, result in altered structural surface parameters, which may be detected using XRD [62], Raman [63], or FTIR [64].

Alternatively, other innovative techniques to investigate the intermediates may be pursued to understand the eNRR process. The well-established fluorescence-based imaging techniques have already been shown to be valuable tools for studying mechanisms in biochemistry [65] and may help to solve the eNRR conundrum. Siddharth and colleagues [66] recently demonstrated the successful use of an 'aggregation-induced emission (AIE) luminogen' to detect the hydrazine (N<sub>2</sub>H<sub>4</sub>) intermediate in the ammonia oxidation reaction. This new concept has a great potential for capturing elusive eNRR intermediates as they appear on the surface [66].

### Concluding remarks

The rapid surge in eNRR research has fueled the widescale testing of many materials/systems as catalyst candidates; however, only a few possess the qualifications for further consideration. Lingering doubts on the feasibility of eNRR in aqueous electrolytes have prompted some re-evaluations on earlier-stage eNRR research [13,14,67] affected by Nr. While a few queries have been substantiated by more assiduous investigation with <sup>15</sup>N<sub>2</sub> isotopic labeling and newly discovered Nr sources [13], some reported eNRR systems remain highly debatable due to the remarkable inconsistency in eNRR performances. Time will ultimately settle the debates, though the path may be tortuous.

In the authors' opinion, further advancement of eNRR is bottlenecked by the lack of a widely agreed 'benchmarking performance' from a well-established proven catalytic system, which can endure repeatable examinations by individual research groups under commonly accessible testing conditions (see [Outstanding questions](#)). The quest for benchmarking performance requires scientific rigor in conducting eNRR research, transparency in material handling and data reporting, and effective cross-laboratory communications to improve experimental reproducibility.

The achievement of such a goal can be substantially facilitated by the development of ultrafast and ultrasensitive analytical methods for NH<sub>3</sub> quantification [68,69], convenient and affordable

### Outstanding questions

Given that the nitrate/nitrite reduction reaction and eNRR share the same N<sub>2</sub>H<sub>y</sub> moieties as intermediates, how do we ascertain which reaction the detected intermediates belong to?

The eNRR performance is largely limited by the low concentration of N<sub>2</sub> in most eNRR electrolytes because of the poor solubility. What engineering strategies can be conveniently adopted to increase the availability of N<sub>2</sub> in an electrolytic cell effectively?

Can we find a set of widely accepted 'benchmarking eNRR performances', from each category of the reported eNRR catalysts under commonly accessible conditions, as experimental guidance for future catalyst evaluation?

In addition to NH<sub>3</sub>, what other N-containing products can we electrochemically synthesize by broadening the eNRR process in conjunction with other established processes and how can we properly design the control experiments to confirm the N source of those products unambiguously?

What anodic reactions can we pair with the eNRR cathode to achieve low energy consumption and high system efficiency? Is it possible to directly synthesize ammonium nitrite/nitrate in one electrochemical reactor by coupling the eNRR process with mild-condition N<sub>2</sub> oxidation?

platforms for standardized evaluation of eNRR performance (e.g., the gas circulation system suggested herein), and advanced *in situ/ex situ* characterization techniques to reliably identify reaction pathways. We stress that it is also crucial to remain neutral and unbiased towards positive and negative results, although they may be contradictory. After all, 'Absence of evidence is not evidence of absence' (Martin Rees).

Besides catalyst development, improvement in the reactor design should be considered to ameliorate the eNRR process. For instance, a membrane electrode assembly (MEA)-based electrolyzer with a hydrophobic GDE can increase the mass-transfer-limited current density of eNRR and allow effective regulation of water content [36]. Systems with anion-exchange membranes appear more promising than proton-exchange membranes owing to less competition from HER. Any future exercise in these systems should prioritize and be based on the  $^{15}\text{N}_2$  control experiment with the gas circulation installation to eliminate the impact of  $\text{N}_2$ ; impacts of other factors such as relative humidity, the hydrophobicity/porosity of the electrode, temperature, and pressure, along with the possible interference on the  $\text{NH}_3$  quantification methods, warrant meticulous and thorough investigation. Some existing eNRR work in GDE-based electrolyzers is summarized in Table S2 in the supplemental information online.

The state-of-the-art eNRR systems remain far from being sufficiently competitive as a qualified candidate for commercial-scale  $\text{NH}_3$  synthesis. The synergistic combination of reliable experimental and theoretical studies, powerful characterization instruments, and robust design of reactors may offer bright and exciting prospects for eNRR research, thereby expediting the N-centric chemical industries towards a renewable-energy-driven future.

### Acknowledgments

The authors acknowledge the support from the Research Grant Council (16308420 and 16310419), Innovation and Technology Commission (grant no. ITC-CNERC14EG03), of the Hong Kong Special Administrative Region, the Southern Marine Science and Engineering Guangdong Laboratory (Guangzhou) (Guangzhou) (SMSEGL20SC01), and the National Science Foundation under grant no. CHE-2036944. We appreciate Dr Jacek A. Koziel and Myeongseong Lee at Iowa State University for their generous assistance in  $\text{N}_2\text{O}$  measurement. W.L. acknowledges his Herbert L. Stiles Faculty Fellowship. U.B.S. acknowledges his Hong Kong PhD Fellowship.

### Declaration of interests

The authors declare no interests.

### Supplemental information

Supplemental information associated with this article can be found online at <https://doi.org/10.1016/j.trechm.2021.11.007>.

### References

1. Smil, V. (2001) *Enriching the Earth. Fritz Haber, Carl Bosch, and the Transformation of World Food Production*. MIT Press
2. Davies-Barnard, T. and Friedlingstein, P. (2020) The global distribution of biological nitrogen fixation in terrestrial natural ecosystems. *Glob. Biogeochem. Cycles* 34, e2019GB006387
3. US Geological Survey (2021) *Mineral commodity summaries 2021*, US Geological Survey
4. Foster, S.L. *et al.* (2018) Catalysts for nitrogen reduction to ammonia. *Nat. Catal.* 1, 490–500
5. MacFarlane, D.R. *et al.* (2020) A roadmap to the ammonia economy. *Joule* 4, 1186–1205
6. Chen, J.G. *et al.* (2018) Beyond fossil fuel-driven nitrogen transformations. *Science* 360, eaar6611
7. Martin, A.J. *et al.* (2019) Electrocatalytic reduction of nitrogen: from Haber–Bosch to ammonia artificial leaf. *Chem* 5, 263–283
8. Soloveichik, G. (2019) Electrochemical synthesis of ammonia as a potential alternative to the Haber–Bosch process. *Nat. Catal.* 2, 377–380
9. Tsuneto, A. *et al.* (1994) Lithium-mediated electrochemical reduction of high pressure  $\text{N}_2$  to  $\text{NH}_3$ . *J. Electroanal. Chem.* 367, 183–188
10. Andersen, S.Z. *et al.* (2020) Increasing stability, efficiency, and fundamental understanding of lithium-mediated electrochemical nitrogen reduction. *Energy Environ. Sci.* 13, 4291–4300
11. Hu, B. *et al.* (2019) Electrochemical dinitrogen reduction to ammonia by  $\text{Mo}_2\text{N}$ : catalysis or decomposition? *ACS Energy Lett.* 4, 1053–1054
12. Du, H.-L. *et al.* (2020) Is molybdenum disulfide modified with molybdenum metal catalytically active for the nitrogen reduction reaction? *J. Electrochem. Soc.* 167, 146507

13. Chen, Y. *et al.* (2020) Revealing nitrogen-containing species in commercial catalysts used for ammonia electrosynthesis. *Nat. Catal.* 3, 1055–1061
14. Choi, J. *et al.* (2020) Identification and elimination of false positives in electrochemical nitrogen reduction studies. *Nat. Commun.* 11, 5546
15. Suryanto, B.H.R. *et al.* (2019) Challenges and prospects in the catalysis of electroreduction of nitrogen to ammonia. *Nat. Catal.* 2, 290–296
16. Andersen, S.Z. *et al.* (2019) A rigorous electrochemical ammonia synthesis protocol with quantitative isotope measurements. *Nature* 570, 504–508
17. Chen, G.-F. *et al.* (2019) Advances in electrocatalytic N<sub>2</sub> reduction—strategies to tackle the selectivity challenge. *Small Methods* 3, 1800337
18. Chen, A. and Xia, B.Y. (2019) Ambient dinitrogen electrocatalytic reduction for ammonia synthesis. *J. Mater. Chem. A* 7, 23416–23431
19. Qing, G. *et al.* (2020) Recent advances and challenges of electrocatalytic N<sub>2</sub> reduction to ammonia. *Chem. Rev.* 120, 5437–5516
20. Greenlee, L.F. *et al.* (2018) The use of controls for consistent and accurate measurements of electrocatalytic ammonia synthesis from dinitrogen. *ACS Catal.* 8, 7820–7827
21. Choi, J. *et al.* (2020) Electroreduction of nitrates, nitrites, and gaseous nitrogen oxides: a potential source of ammonia in dinitrogen reduction studies. *ACS Energy Lett.* 5, 2095–2097
22. Long, J. *et al.* (2020) Direct electrochemical ammonia synthesis from nitric oxide. *Angew. Chem. Int. Ed.* 59, 9711–9718
23. Li, P. *et al.* (2021) A single-site iron catalyst with preoccupied active centers that achieves selective ammonia electrosynthesis from nitrate. *Energy Environ. Sci.* 14, 3522–3531
24. Yu, W. *et al.* (2020) Cathodic NH<sub>4</sub><sup>+</sup> leaching of nitrogen impurities in CoMo thin-film electrodes in aqueous acidic solutions. *Sustain. Energy Fuels* 4, 5080–5087
25. Dabundo, R. *et al.* (2014) The contamination of commercial <sup>15</sup>N<sub>2</sub> gas stocks with <sup>15</sup>N-labeled nitrate and ammonium and consequences for nitrogen fixation measurements. *PLoS One* 9, e110335
26. Li, L. *et al.* (2019) Electrochemical nitrogen reduction: identification and elimination of contamination in electrolyte. *ACS Energy Lett.* 4, 2111–2116
27. Liu, H. *et al.* (2020) The removal of inevitable NO<sub>x</sub> species in catalysts and the selection of appropriate membrane for measuring electrocatalytic ammonia synthesis accurately. *J. Energy Chem.* 49, 51–58
28. Tang, C. and Qiao, S.-Z. (2019) How to explore ambient electrocatalytic nitrogen reduction reliably and insightfully. *Chem. Soc. Rev.* 48, 3166–3180
29. Burris, R.H. (1972) Nitrogen fixation – assay methods and techniques. In *Photosynthesis and Nitrogen Fixation Part B* (Vol. 24), pp. 415–431, Academic Press
30. Dandekar, A. and Vannice, M.A. (1999) Decomposition and reduction of N<sub>2</sub>O over copper catalysts. *Appl. Catal. B Environ.* 22, 179–200
31. Wang, M. *et al.* (2021) Salting-out effect promoting highly efficient ambient ammonia synthesis. *Nat. Commun.* 12, 3198
32. Chou, S.-S. *et al.* (2003) A high performance liquid chromatography method for determining nitrate and nitrite levels in vegetables. *J. Food Drug Anal.* 11, 233–238
33. Carvalho, A.P. *et al.* (1998) Rapid spectrophotometric determination of nitrates and nitrites in marine aqueous culture media. *Analyst* 26, 347–351
34. Suryanto, B.H.R. *et al.* (2021) Nitrogen reduction to ammonia at high efficiency and rates based on a phosphonium proton shuttle. *Science* 372, 1187–1191
35. Mohr, W. *et al.* (2010) Methodological underestimation of oceanic nitrogen fixation rates. *PLoS One* 5, e12583
36. Rabiee, H. *et al.* (2021) Gas diffusion electrodes (GDEs) for electrochemical reduction of carbon dioxide, carbon monoxide, and dinitrogen to value-added products: a review. *Energy Environ. Sci.* 14, 1959–2008
37. Nielander, A.C. *et al.* (2020) Readily constructed glass piston pump for gas recirculation. *ACS Omega* 5, 16455–16459
38. Robb, W.L. (1968) Thin silicone membranes – their permeation properties and some applications. *Ann. N. Y. Acad. Sci.* 146, 119–137
39. Liu, S. *et al.* (2019) Facilitating nitrogen accessibility to boron-rich covalent organic frameworks via electrochemical excitation for efficient nitrogen fixation. *Nat. Commun.* 10, 3898
40. Wang, M. *et al.* (2020) Unveiling the essential nature of Lewis basicity in thermodynamically and dynamically promoted nitrogen fixation. *Adv. Funct. Mater.* 30, 2001244
41. Lv, X.-W. *et al.* (2021) Iron-doped titanium dioxide hollow nanospheres for efficient nitrogen fixation and Zn–N<sub>2</sub> aqueous batteries. *J. Mater. Chem. A* 9, 4026–4035
42. Liu, S. *et al.* (2021) Proton-filtering covalent organic frameworks with superior nitrogen penetration flux promote ambient ammonia synthesis. *Nat. Catal.* 4, 322–331
43. Yao, Y. *et al.* (2018) A spectroscopic study on the nitrogen electrochemical reduction reaction on gold and platinum surfaces. *J. Am. Chem. Soc.* 140, 1496–1501
44. Yao, Y. *et al.* (2019) Electrochemical nitrogen reduction reaction on ruthenium. *ACS Energy Lett.* 4, 1336–1341
45. Yao, Y. *et al.* (2020) A spectroscopic study of electrochemical nitrogen and nitrate reduction on rhodium surfaces. *Angew. Chem. Int. Ed.* 59, 10479–10483
46. Liu, S. *et al.* (2020) Altering the rate-determining step over cobalt single clusters leading to highly efficient ammonia synthesis. *Natl. Sci. Rev.* 8, nwa136
47. Wang, M. *et al.* (2019) Over 56.55% Faradaic efficiency of ambient ammonia synthesis enabled by positively shifting the reaction potential. *Nat. Commun.* 10, 341
48. Wang, Z. *et al.* (2021) Efficient nitrogen reduction to ammonia by fluorine vacancies with a multi-step promoting effect. *J. Mater. Chem. A* 9, 894–899
49. Zeinalipour-Yazdi, C.D. *et al.* (2015) Nitrogen activation in a Mars–van Krevelen mechanism for ammonia synthesis on Co<sub>3</sub>Mo<sub>3</sub>N. *J. Phys. Chem. C* 119, 28368–28376
50. Abghoui, Y. *et al.* (2015) Enabling electrochemical reduction of nitrogen to ammonia at ambient conditions through rational catalyst design. *Phys. Chem. Chem. Phys.* 17, 4909–4918
51. Abghoui, Y. and Skúlason, E. (2017) Electrochemical synthesis of ammonia via Mars–van Krevelen mechanism on the (111) facets of group III–VII transition metal mononitrides. *Catal. Today* 286, 78–84
52. Yang, X. *et al.* (2018) Mechanistic insights into electrochemical nitrogen reduction reaction on vanadium nitride nanoparticles. *J. Am. Chem. Soc.* 140, 13387–13391
53. Nash, J. *et al.* (2019) Elucidation of the active phase and deactivation mechanisms of chromium nitride in the electrochemical nitrogen reduction reaction. *J. Phys. Chem. C* 123, 23967–23975
54. Zhang, X. *et al.* (2018) Highly efficient electrochemical ammonia synthesis via nitrogen reduction reactions on a VN nanowire array under ambient conditions. *Chem. Commun.* 54, 5323–5325
55. Zhang, R. *et al.* (2018) High-efficiency electrosynthesis of ammonia with high selectivity under ambient conditions enabled by VN nanosheet array. *ACS Sustain. Chem. Eng.* 6, 9545–9549
56. Yang, X. *et al.* (2019) Quantification of active sites and elucidation of the reaction mechanism of the electrochemical nitrogen reduction reaction on vanadium nitride. *Angew. Chem.* 131, 13906–13910
57. Shahid, U.B. *et al.* (2021) Electrifying the nitrogen cycle: an electrochemical endeavor. *Curr. Opin. Electrochem.* 30, 100790
58. Nayak, S. *et al.* (2018) Adsorbed intermediates in oxygen reduction on platinum nanoparticles observed by *in situ* IR spectroscopy. *Angew. Chem. Int. Ed.* 57, 12855–12858
59. Smith, B.C. (2011) *Fundamentals of Fourier Transform Infrared Spectroscopy*. CRC Press
60. Nakata, K. *et al.* (2008) Surface-enhanced infrared absorption spectroscopic studies of adsorbed nitrate, nitric oxide, and related compounds 2: nitrate ion adsorption at a platinum electrode. *Langmuir* 24, 4358–4363
61. Milella, F. and Mazzotti, M. (2019) Estimating speciation of aqueous ammonia solutions of ammonium bicarbonate: application of least squares methods to infrared spectra. *React. Chem. Eng.* 4, 1284–1302

62. Gabunia, D. *et al.* (2009) Isotopic composition dependences of lattice constant and thermal expansion of  $\beta$ -rhombohedral boron. *J. Phys. Conf. Ser.* 176, 012022
63. Muhamadali, H. *et al.* (2015) Combining Raman and FT-IR spectroscopy with quantitative isotopic labeling for differentiation of *E. coli* cells at community and single cell levels. *Anal. Chem.* 87, 4578–4586
64. Kira, O. *et al.* (2014) A novel method combining FTIR-ATR spectroscopy and stable isotopes to investigate the kinetics of nitrogen transformations in soils. *Soil Sci. Soc. Am. J.* 78, 54–60
65. Chen, Y. *et al.* (2019) Aggregation-induced emission: fundamental understanding and future developments. *Mater. Horiz.* 6, 428–433
66. Siddharth, K. *et al.* (2021) Hydrazine detection during ammonia electro-oxidation using an aggregation-induced emission dye. *J. Am. Chem. Soc.* 143, 2433–2440
67. Shipman, M.A. and Symes, M.D. (2017) A re-evaluation of Sn(II) phthalocyanine as a catalyst for the electrosynthesis of ammonia. *Electrochim. Acta* 258, 618–622
68. Yu, W. *et al.* (2020) Isotopically selective quantification by UPLC-MS of aqueous ammonia at submicromolar concentrations using dansyl chloride derivatization. *ACS Energy Lett.* 5, 1532–1536
69. Liu, Y. *et al.* (2020) Facile all-optical method for in situ detection of low amounts of ammonia. *iScience* 23, 101757
70. Fichter, Fr. *et al.* (1930) Elektrolytische Bindung von komprimiertem Stickstoff bei gewöhnlicher Temperatur. *Helv. Chim. Acta* 13, 1228–1236 (in German)
71. Tsuneto, A. *et al.* (1993) Efficient electrochemical reduction of  $N_2$  to  $NH_3$  catalyzed by lithium. *Chem. Lett.* 22, 851–854
72. McEnaney, J.M. *et al.* (2017) Ammonia synthesis from  $N_2$  and  $H_2O$  using a lithium cycling electrification strategy at atmospheric pressure. *Energy Environ. Sci.* 10, 1621–1630
73. Lazouski, N. *et al.* (2019) Understanding continuous lithium-mediated electrochemical nitrogen reduction. *Joule* 3, 1127–1139
74. Lazouski, N. *et al.* (2020) Non-aqueous gas diffusion electrodes for rapid ammonia synthesis from nitrogen and water-splitting-derived hydrogen. *Nat. Catal.* 3, 463–469
75. Ito, Y. and Goto, T. (1997) The electrochemical reduction of  $N_2$  gas and its application to energy systems. In *IECEC-97 proceedings of the Thirty-Second Intersociety Energy Conversion Engineering Conference*, pp. 787–792, IEEE
76. McPherson, I.J. *et al.* (2019) The feasibility of electrochemical ammonia synthesis in molten LiCl–KCl eutectics. *Angew. Chem. Int. Ed.* 58, 17433–17441
77. Licht, S. *et al.* (2020) Retraction. *Science* 369, 780
78. Choi, J. *et al.* (2020) Promoting nitrogen electroreduction to ammonia with bismuth nanocrystals and potassium cations in water. *ChemRxiv* Published online January 31, 2020. <https://doi.org/10.26434/chemrxiv.11768814>
79. Manjunatha, R. *et al.* (2020) Electrochemical and chemical instability of vanadium nitride in the synthesis of ammonia directly from nitrogen. *ChemCatChem* 12, 438–443
80. Du, H.-L. *et al.* (2019) Critical assessment of the electrocatalytic activity of vanadium and niobium nitrides toward dinitrogen reduction to ammonia. *ACS Sustain. Chem. Eng.* 7, 6839–6850
81. Hao, Y.-C. *et al.* (2019) Promoting nitrogen electroreduction to ammonia with bismuth nanocrystals and potassium cations in water. *Nat. Catal.* 2, 448–456
82. Yao, D. *et al.* (2020) *In situ* fragmented bismuth nanoparticles for electrocatalytic nitrogen reduction. *Adv. Energy Mater.* 10, 2001289
83. Li, L. *et al.* (2019) Two-dimensional mosaic bismuth nanosheets for highly selective ambient electrocatalytic nitrogen reduction. *ACS Catal.* 9, 2902–2908
84. Wang, Y. *et al.* (2019) Generating defect-rich bismuth for enhancing the rate of nitrogen electroreduction to ammonia. *Angew. Chem. Int. Ed.* 58, 9464–9469
85. Xia, L. *et al.* (2020) Engineering abundant edge sites of bismuth nanosheets toward superior ambient electrocatalytic nitrogen reduction via topotactic transformation. *ACS Sustain. Chem. Eng.* 8, 2735–2741
86. Mukherjee, S. *et al.* (2018) Metal–organic framework-derived nitrogen-doped highly disordered carbon for electrochemical ammonia synthesis using  $N_2$  and  $H_2O$  in alkaline electrolytes. *Nano Energy* 48, 217–226
87. Zhao, Y. *et al.* (2019) Ammonia detection methods in photocatalytic and electrocatalytic experiments: how to improve the reliability of  $NH_3$  production rates? *Adv. Sci.* 6, 1802109
88. Iriawan, H. *et al.* (2021) Methods for nitrogen activation by reduction and oxidation. *Nat. Rev. Methods Primers* 1, 56
89. Zhou, F. *et al.* (2017) Electro-synthesis of ammonia from nitrogen at ambient temperature and pressure in ionic liquids. *Energy Environ. Sci.* 10, 2516–2520
90. Wang, H. *et al.* (2019) Selective electrochemical reduction of nitrogen to ammonia by adjusting the three-phase interface. *Research* 2019, 1401209
91. Tan, L. *et al.* (2019) Synthesis of ammonia via electrochemical nitrogen reduction on high-index faceted Au nanoparticles with a high Faradaic efficiency. *Chem. Commun.* 55, 14482–14485
92. Xue, Z.-H. *et al.* (2019) Electrochemical reduction of  $N_2$  into  $NH_3$  by donor–acceptor couples of Ni and Au nanoparticles with a 67.8% Faradaic efficiency. *J. Am. Chem. Soc.* 141, 14976–14980
93. Du, C. *et al.* (2019) Achieving 59% faradaic efficiency of the  $N_2$  electroreduction reaction in an aqueous Zn– $N_2$  battery by facilely regulating the surface mass transport on metallic copper. *Chem. Commun.* 55, 12801–12804
94. Peng, G. *et al.* (2020) Nitrogen-defective polymeric carbon nitride nanolayer enabled efficient electrocatalytic nitrogen reduction with high Faradaic efficiency. *Nano Lett.* 20, 2879–2885
95. Liu, Y. *et al.* (2020) Coupling Cu with Au for enhanced electrocatalytic activity of nitrogen reduction reaction. *Nanoscale* 12, 1811–1816
96. Fang, Y. *et al.* (2020) Graphdiyne interface engineering: highly active and selective ammonia synthesis. *Angew. Chem. Int. Ed.* 59, 13021–13027
97. Zhang, S. *et al.* (2020) Electrocatalytically active Fe–(O–C<sub>2</sub>)<sub>4</sub> single-atom sites for efficient reduction of nitrogen to ammonia. *Angew. Chem. Int. Ed.* 59, 13423–13429
98. Liu, Y. *et al.* (2020) A highly efficient metal-free electrocatalyst of F-doped porous carbon toward  $N_2$  electroreduction. *Adv. Mater.* 32, 1907690
99. Wang, X. *et al.* (2020) Polyoxometalate-based metal–organic framework-derived bimetallic hybrid materials for upgraded electrochemical reduction of nitrogen. *Green Chem.* 22, 6157–6169
100. Guo, Y. *et al.* (2020) A rechargeable Al– $N_2$  battery for energy storage and highly efficient  $N_2$  fixation. *Energy Environ. Sci.* 13, 2888–2895
101. Haynes, W.M. (2016) CRC Handbook of Chemistry and Physics. CRC Press
102. Maurer, D.L. *et al.* (2017) Farm-scale testing of soybean peroxidase and calcium peroxide for surficial swine manure treatment and mitigation of odorous VOCs, ammonia and hydrogen sulfide emissions. *Atmos. Environ.* 166, 467–478
103. Kozawa, A. and Kordesch, K.V. (1981) Silver-catalysed  $MnO_2$  as hydrogen absorber. *Electrochim. Acta* 26, 1489–1493
104. Edwards, J.D. and Pickering, S.F. (1920) Permeability of Rubber to Gases (No. 387). US Government Printing Office
105. Wang, Y. *et al.* (2021) Nitrate electroreduction: mechanism insight, *in situ* characterization, performance evaluation, and challenges. *Chem. Soc. Rev.* 50, 6720–6733
106. Yao, Y. *et al.* (2020) Electrochemical synthesis of ammonia from nitrogen under mild conditions: current status and challenges. *Electrochem. Energy Rev.* 3, 239–270
107. Matsui, T. *et al.* (2015) *In situ* attenuated total reflection infrared spectroscopy on electrochemical ammonia oxidation over Pt electrode in alkaline aqueous solutions. *Langmuir* 31, 11717–11723
108. Jin, L. and Seifitokaldani, A. (2020) *In situ* spectroscopic methods for electrocatalytic  $CO_2$  reduction. *Catalysts* 10, 481